

## Laminar Natural Convection Study in a Horizontal Half-Elliptical Enclosure Using Heater on Horizontal Wall

Abdelkarim Bouras<sup>1,3</sup>, Djedid Taloub<sup>1,2,\*</sup>, Abdelhadi Beghidja<sup>2</sup>, Zied Driss<sup>4</sup>

<sup>1</sup> Department of Physics, Faculty of Sciences, University MohamedBoudiaf of M'sila, M'sila, Algeria

<sup>2</sup> Laboratory of Renewable Energy and Sustainable Development (LRES), University brothers Mentouri Constantine1, Algeria

<sup>3</sup> Laboratory of Energetic Physics, University brothers Mentouri Constantine1, Constantine1, Algeria

<sup>4</sup> Laboratory of Electromechanical Systems (LASEM), National School of Engineers of Sfax (ENIS), University of Sfax, Sfax, Tunisia

### ARTICLE INFO

#### Article history:

Received 12 October 2018

Received in revised form 29 December 2018

Accepted 2 January 2019

Available online 11 January 2019

### ABSTRACT

A numerical analysis of laminar natural convection in a horizontal annulus between an internal heated plane and an external cold half-elliptical was investigated using approximation of Boussinesq. Both internal and external walls are maintained at the constant temperature and air is the working fluid. Numerical solutions are obtained using a commercial computational fluid dynamics package, FLUENT, using the finite volume method. Effects of the Rayleigh number,  $Rat$ , on the Nusselt number,  $Nu$ , as well as velocity and temperature fields are investigated for the range of  $Rat$  from 1.0 10<sup>3</sup> to 5.0 10<sup>5</sup>. The results show that for a small thermal Rayleigh number, the heat transfer within the annulus is essentially controlled by the conduction process. As the thermal Rayleigh number increases ( $Rat \geq 104$ ), the role of convection becomes predominant. Also the heat transfer rate increases. The aim of this study is to observe the effects of thermal Rayleigh number on the structure of the flow and the distribution of the temperature.

#### Keywords:

Thermal transfer, Natural convection,  
Circular and half-elliptical, Multicellular  
flow, Laminar flow, Steady flow.

Copyright © 2019 PENERBIT AKADEMIA BARU - All rights reserved

## 1. Introduction

The determination of heat transfer and flow characteristics generated by the forces of Archimedes in cavity is a problem whose interest so much on the fundamental plane than on the level of the practical applications is important for purpose of cooling or heating in industry. Among these applications, we can quote the storage of the fluids, the heat exchangers, and the flow of air in the rooms and in the solar collectors. It arises from available works in the literature, very little information is currently available so much on the numerical studies than experimental, on the structure flow of natural convection occurring in a half-elliptical cavity, like the natural flow of the air in the agricultural greenhouses, in elliptical hangars or the cockpits of the airliners.

\* Corresponding author.

E-mail address: [djtaloub@gmail.com](mailto:djtaloub@gmail.com) (Djedid Taloub)

A very large number of works on the natural convection in cavity of different geometry while passing from the rectangular cavity. Was studied a numerical study on buoyancy-driven laminar flow in an inclined square enclosure heated from one side and cooled from the adjacent side was conducted using finite difference methods for example. Aydin *et al.* [1] Focused on the basis of the numerical data. They determined the critical values of the inclination angle at which the rate of heat transfer within the enclosure is either maximum or minimum. Rahman *et al.* [2] conducted numerical investigations, on the convection strength which increases as the enclosure shape changes from slender through square to shallow at any particular inclination, and varies mildly with inclination at a particular aspect ratio. Deng *et al.* [3] simulated natural convection heat transfer in a rectangular cavity heated from below and uniformly cooled from the top and both sides. The integral forms of the governing equations were solved numerically using the finite-volume method in a non-orthogonal body-fitted coordinate system. Moukalled and Acharya [4] solved the governing equations of natural convection heat transfer inside a trapezoidal shaped geometry with baffles for building roofs in the conditions of summerlike and winter-like. They observed that in winter-like conditions, convection starts to dominate at a Rayleigh number much lower than that in summerlike conditions. Numerical investigation of natural convection heat transfer in a rectangular enclosure with sinusoidal temperature distributions on both side walls and upper walls was investigated by many authors [5, 6].

Triangular shaped enclosures were investigated by some authors, where, numerical and experimental studies of steady-state natural convection in triangular enclosures were performed by Oztopa [7]. Numerically, they used finite difference method approach to solve the governing equations for laminar natural convective heat transfer. The experimental and numerical results showed good agreement. Indeed, they observed that the inclination angle can be used as a control parameter for heat transfer. A numerical study on heat distribution and thermal mixing during steady laminar natural convective flow inside a right-angled triangular enclosure filled with porous media subjected to various wall boundary conditions using Bejan's heat lines approach was investigated by Ram [8]. As analytical solution, numerical use of the FLUENT/UNS code and experimental studies of laminar heat transfer from an isothermal hemispherical cavity in unlimited space were presented by Jawad [9]. The comparison of theoretical and numerical solutions with experimental results presented good agreement. In tilted hemispherical cavities, Bāiri *et al.* [10] studied numerically and experimentally the state free convection generated by constant heat flux in tilted hemispherical cavities. The Rayleigh number resulting from the experimental parameters varies between  $3.44 \cdot 10^5$  and  $2.83 \cdot 10^7$ . The numerical study covered a larger  $Ra_t$  range, between  $10^4$  and  $5 \cdot 10^7$ . The resulting thermal and dynamic fields were presented for all the angles treated. Correlations between average Nusselt and Rayleigh numbers were proposed to quantify the convective exchanges for engineering applications. Saber *et al.* [11] investigated steady natural convection heat transfer in hemispherical cavities with horizontal plane. The numerical model was based on the finite element method. The results show that for different boundary temperature conditions, the airflow in the cavities is mono-cellular. The results were used to develop correlations for the Nusselt number. The natural convection in a quadrantal cavities were studied by different authors, where, an experimental and numerical study in a water-filled quadrantal cavity heated and cooled on adjacent walls was announced by Aydin and Yesiloz [12] and for inclined quadrantal cavity was reported by Aydin and Yesiloz [13]. Sen *et al.* [14] investigated numerically the buoyancy-induced flow and heat transfer mechanisms in a water-filled quadrantal cavity from the heaters attached on both the vertical and horizontal walls, while curved wall is cold. Effects of the Rayleigh number, on the Nusselt number, as well as velocity and temperature fields are investigated for the range of  $Ra_t$  from  $10^3$  to  $10^7$ . They observed that the heat transfer increases with increase in Rayleigh number. Retiel *et al.* [15] studied

the effects of the thermal Rayleigh number ( $10^3 \leq Ra_t \leq 10^5$ ) and of the Lewis number ( $0.5 \leq Le \leq 5$ ) on the double-diffusive natural convection in a closed horizontal half-cylindrical cavity, for report/ratio of the thermal Rayleigh and solutal.

According to these results, it is clear that the study of the natural convection has been studied by deferent authors, however, the half-elliptical enclosure has evoked considerable interest, a detailed numerical study of flow and heat transfer in half-ellipse is useful in including the processes that occur in natural convection flows in agricultural greenhouse, in elliptical hangar, cockpit of the airliner, design off solar air heating system etc.

Particularly, as, we propose to studies the effect of the thermal Rayleigh number in the range of  $10^3 \leq Ra_t \leq 5 \cdot 10^5$  on the natural convection in a closed horizontal half-elliptic cavity from the heater attached on horizontal wall, while curved wall is cold, where the Prandtl number fixed at 0.71. The aim of this study is to observe the effects of Rayleigh number on the structure of the flow and the distribution of the temperature.

## 2. Physical Model and Mathematical Formulation

### 2.1 Description of The Problem

Figure 1 shows a cross section of the system. In this system, we consider a half-elliptic cavity closed and contains an incompressible fluid of kinematic viscosity  $\nu$  and of thermal diffusivity  $\alpha$ . The higher wall “ceiling” and the lower wall “the floor” generate a vertical variation in temperature (active walls). The elliptical annular space characterized by the eccentricity ( $e=0.7$ ).

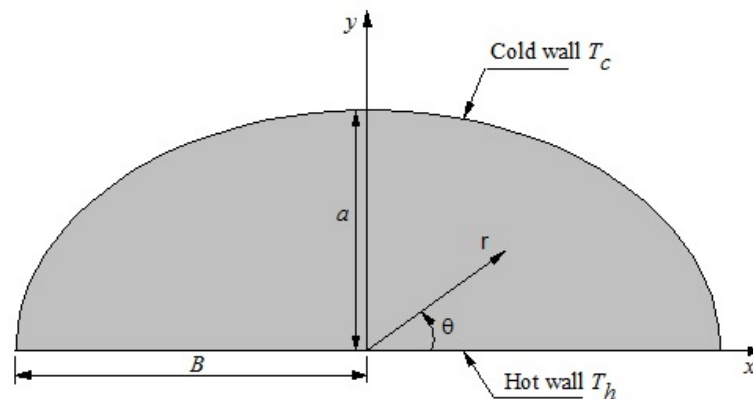


Fig. 1. Schematic presentation of the physical model

### 2.2 Mathematical formulation

A mathematical formulation of the convective flow and heat transfer of fluid is obtained by making the following assumptions: (a) the fluid is Newtonian, (b) the flow is two-dimensional, steady and laminar, (c) the fluid is incompressible with constant properties evaluated at the reference temperature, (d) the viscous dissipation is neglected, and (e) the Boussinesq approximation is used to consider buoyancy. The governing equations inside the half-elliptic enclosure with a heated the lower wall “the floor” are described by the Navier–Stokes and the energy equations, respectively. The governing equations in a cartesian coordinate system are transformed into dimensionless forms under the following non-dimensional variables.

The continuity equation is written as follows (Eq. 1):

$$\frac{\partial U}{\partial X} + \frac{\partial V}{\partial Y} = 0 \quad (1)$$

The momentum equations are written as follows (Eq. 2 and Eq.3)

$$U \frac{\partial U}{\partial X} + V \frac{\partial U}{\partial Y} = -\frac{\partial P}{\partial X} + Pr \left( \frac{\partial^2 U}{\partial X^2} + \frac{\partial^2 U}{\partial Y^2} \right) \quad (2)$$

$$U \frac{\partial V}{\partial X} + V \frac{\partial V}{\partial Y} = -\frac{\partial P}{\partial Y} + Pr \left( \frac{\partial^2 V}{\partial X^2} + \frac{\partial^2 V}{\partial Y^2} \right) + RaPr\theta \quad (3)$$

The energy equation is written as follows (Eq. 4):

$$U \frac{\partial \theta}{\partial X} + V \frac{\partial \theta}{\partial Y} = \left( \frac{\partial^2 \theta}{\partial X^2} + \frac{\partial^2 \theta}{\partial Y^2} \right) \quad (4)$$

The initial conditions are (Eq. 5 and Eq. 6)

$$u = v = 0 \quad (5)$$

$$T = T_0 (= T_e) \quad (6)$$

In addition, the boundary conditions on the system are defined forth  
 Lower plane (Eq. 7 and Eq. 8):

$$u = v = 0 \quad (7)$$

$$T = T_i \quad (8)$$

And forth Half-elliptical ( $0 \leq \theta \leq \pi$ ) (Eq. 9 and Eq. 10)

$$u = v = 0 \quad (9)$$

$$T = T_e \quad (10)$$

The Rayleigh number ( $Ra_t$ ) for the current problem is defined as follows (Eq. 11):

$$Ra_t = \frac{g\beta(T_h - T_c)a^3}{\nu\alpha} \quad (11)$$

The Rayleigh number is defined to base at the distance between the principal axis of the ellipse and the top of half-ellipse.

Local Nusselt number is defined on the characteristic length  $L$  as (Eq. 12):

$$Nu_L = L \left. \frac{\partial \theta}{\partial \vec{n}} \right|_{wall} \quad (12)$$

Where  $\vec{n}$  is the normal vector on the wall and  $\theta$  is the dimensionless temperature.

The length of the horizontal plane (internal)  $P$  and the perimeter of the external half- ellipse  $P_e$  were chosen as a characteristic length  $L$ .

The average Nusselt number external and internal can be evaluated by (Eq. 13 and Eq. 14)

$$\overline{Nu}_i = \frac{1}{P} \int_0^P Nu_L dP \tag{13}$$

$$\overline{Nu}_e = \frac{1}{P_e} \int_0^{P_e} Nu_L dP_e \tag{14}$$

Where  $P$  is the perimeter of the horizontal plane. The average Nusselt number for the two walls of the half-ellipse is defined by (Eq. 15):

$$Nu_{avg} = \frac{\overline{Nu}_e + \overline{Nu}_i}{2} \tag{15}$$

### 2.3 Meshing Choice

In this study, several grids were used arbitrarily for the considered configuration (Figure 2) for  $Ra_t = 1.3 \cdot 10^4$  to observe their effect on the results. Table 1 shows, therefore, the variation of the average Nusselt number, according to the considering nodes. According to these simulations the grid 200 X 200 appears more adequate to choose.

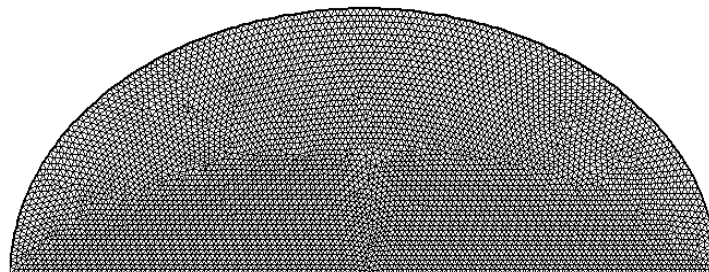


**Fig. 2.** A typical grid distribution (200x200) with uniform and triangular distributions

**Table 1**

Variation of the average Nusselt number according to the number of nodes for  $Ra_t=1.310^4$

Mesh size	140x140	150x150	160x160	180x180	200x200	210x210
Nu (avg)	4,0784	4,0884	4,0955	4,1030	4,1033	4,1035
Relative Error (%)	0.2446	0.1734	0.1828	0.0073	0.0049	

### 3. Numerical Method

The governing equations are solved iteratively by employing the control volume method. The commercial CFD code Fluent 6.3 was used as a solver to study the natural convection heat transfer. The computational domain was generated and meshed in the environment of the preprocessing code Gambit 2.3. Fine structured quadrilateral cells are generated in the thin boundary layers next to the walls. The spatial term in the governing equations are discretized using the Body Force Weighted implicit scheme and the second-order scheme, respectively. The SIMPLE algorithm was used to

implement the pressure- velocity coupling. In addition, the convergence criteria for the velocity components and temperature are set to be  $10^{-4}$  and  $10^{-6}$ , respectively.

## 4. Results and Discussion

The effect of different Rayleigh numbers on the natural convection of heat transfers in the half-elliptic space filled of air ( $Pr = 0.71$ ) was studied for three different Rayleigh numbers. The results were presented as streamlines, isotherms, local and average Nusselt numbers.

### 4.1 Effect of Rayleigh Number

In order to perform the parametric study, three different Rayleigh numbers equal to  $6.1 \cdot 10^3$ ,  $1.3 \cdot 10^4$ , and  $3.1 \cdot 10^5$ , were considered within the laminar convection dominated regime. In this condition, the Prandtl number is fixed at  $Pr = 0.71$  throughout the present study.

Figures 3, 4, 5 and 6 present the isotherms and the streamlines for different values of the thermal Rayleigh number. We notice that these isotherms and these current lines are symmetrical compared with the median fictitious vertical plane. These results show that the diet of the flow is monocellular, on the left side of the symmetry plane. The flow turns in the trigonometrically direction and on the right side, it is contrary direction. The particles of the fluid move upwards under the effect of gravity forces along the internal hot wall then descend near the cold wall of the external half-elliptic.

For  $Ra_t = 6.1 \cdot 10^3$ , the laminar convection is weak. Figure 3 presents the streamlines of the fluid whose flow is organized in two principal cells which rotate very slowly in opposite directions, with a temperature field in the shape of half-ellipse marrying the shape of the cavity. This expresses a weak flow dominated by a thermal diffusion smothered by a stable vertical stratification of temperature. In this case, the temperature distribution decreases from the hot wall to the cold wall (Figure 4).

Indeed, it has been observed that most of the heat transfer is done by conduction on the level of heated wall, although the velocity fields are different from zero. The convection is therefore relatively weak; the values of the current function which are given on the figures are very small.

For  $Ra_t \leq 6.1 \cdot 10^3$ , we are always in pseudo-conductive regime. The heat transfer is done by conduction. The values of the current function are always weak, which reflects relatively weak convection.

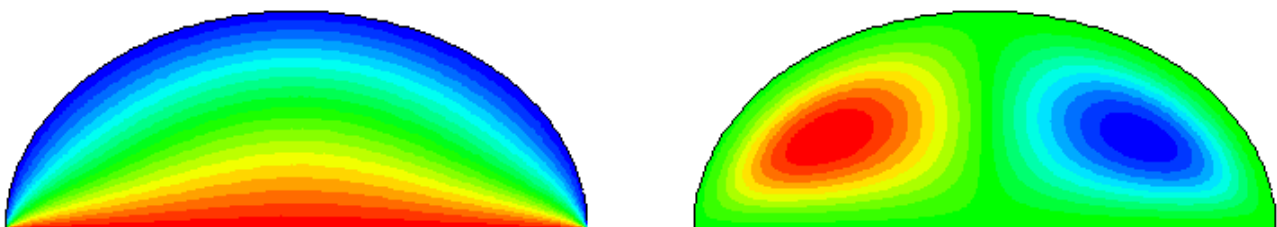
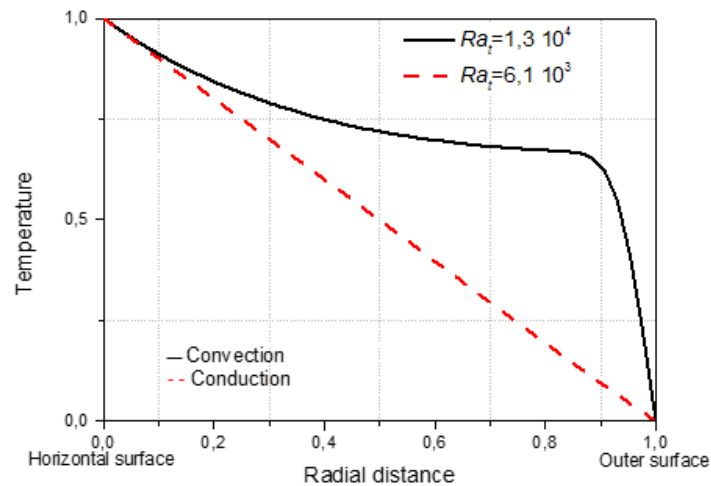


Fig. 3. Isotherms and streamlines for  $Ra_t = 6.1 \cdot 10^3$



**Fig. 4.** Temperature distribution

For  $Ra_t = 1.3 \cdot 10^4$ , the isothermal lines in the Figure 5 are transformed symmetrical compared to the vertical axis and changed significantly. The values of the function current mentioned on the same figure are also significantly increased, which presents an increase in the convection, but remains relatively weak as the appearance of the isothermal lines shows it.

In addition, it has been noted that the thermal diffusivity is more important and have a consequence on the distribution of the temperature. In fact, it has been observed a clear predominance of the thermal stratification in the middle of the cavity (Figure 5). Also, it has been noted that the thermal boundary layers have thin thicknesses in the center of the horizontal cavity, which results an intense heat transfer in the top of the cavity and a weak transfer on the sides.

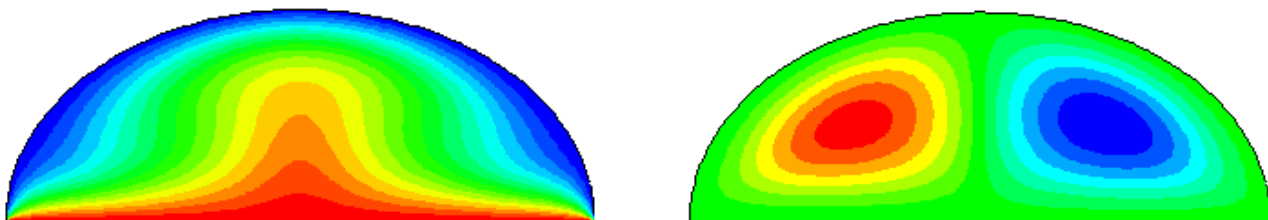


**Fig. 5.** Isotherms and streamlines for  $Ra_t = 1.3 \cdot 10^4$

Figure 6 shows the isotherms and streamlines for  $Ra_t = 3.1 \cdot 10^5$ . According to these results, it is clear that the isothermal lines are changed and eventually adopted the shape of a mushroom. The temperature distribution is decreasing from the hot wall to the cold wall. The direction of the deformation of the isotherms was conformed to the direction of rotation of current lines. In laminar regime, it has been observed that, under the action of the movement of the particles which unstick from the hot wall at the axis of symmetry, the isothermal lines are arched and moving away from the horizontal wall. The values of the current functions increase what means that the convection becomes intensified. The increase in the Rayleigh number intensifies the convection. The superior nodes are reinforced and started to be melted then with those lower, as presented in Figure 6.

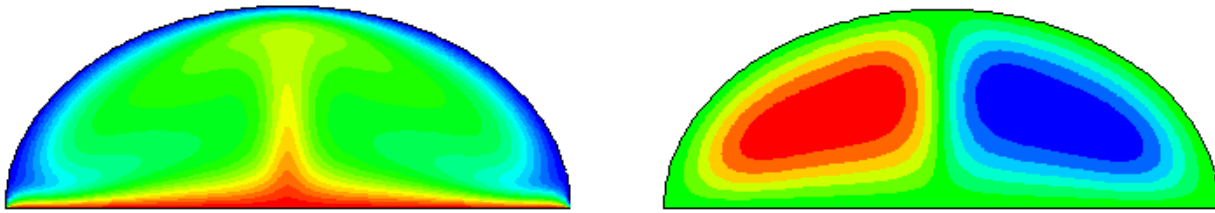


Fig.

6. Isotherms and streamlines for  $Ra_t = 3.1 \cdot 10^5$

#### 4.2 Local Nusselt Number Along the Horizontal Wall

Figure 7 illustrates the evolution of the local Nusselt number  $Nu_i$  on the horizontal wall (hot wall) for different Rayleigh numbers equal to  $Ra_t = 6.1 \cdot 10^3$ ,  $Ra_t = 1.3 \cdot 10^4$ ,  $Ra_t = 3.1 \cdot 10^5$  and  $Ra_t = 5.0 \cdot 10^5$  according to these results, it is clear that with the increase of the Rayleigh number, the value of the local Nusselt number increases, which is obvious. The minimal value is observed at  $\theta = 90^\circ$  However, the maximum values equal to  $Nu_i = 11.25$  are obtained at  $\theta = 0^\circ$  and  $\theta = 180^\circ$ .

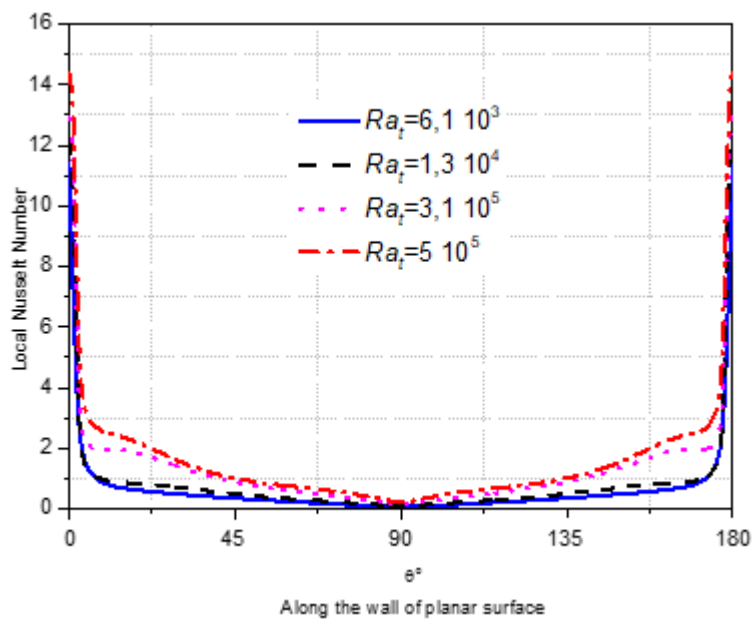
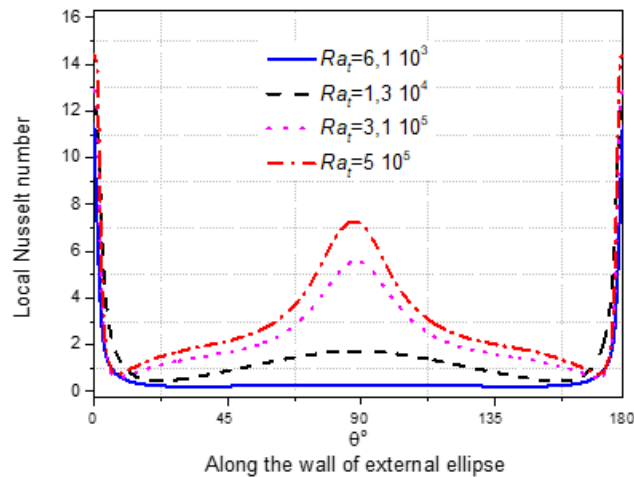


Fig. 7. Variation of the local Nusselt number along the hot wall

#### 4.3 Local Nusselt Number Along the Half-Elliptic Wall

Figure 8 presents the evolution of the local Nusselt number  $Nu_e$  along the external wall for different Rayleigh numbers equal to  $Ra_t = 6.1 \cdot 10^3$ ,  $Ra_t = 1.3 \cdot 10^4$ ,  $Ra_t = 3.1 \cdot 10^5$  and  $Ra_t = 5.0 \cdot 10^5$  according to these results, it is clear that  $Nu_e$  is maximum value in the summit area localized at  $\theta = 90^\circ$  and to the extremes of half-ellipse localized at  $\theta = 0^\circ$  and  $\theta = 180^\circ$  where the fluid is practically motionless.



**Fig. 8.** Variation of the local Nusselt number along the cold wall

#### 4.4 Local Nusselt number on the internal and external walls

Figure 9 presents the variation of the local Nusselt numbers  $Nu_i$  and  $Nu_e$  along the internal and external walls for  $Ra_t = 3.1 \cdot 10^5$ . According to these results, it has been noted that the two contact points between the half-ellipse and the horizontal plane are maximum value. Indeed, it is clear that the local Nusselt number,  $Nu_e$  is maximum value in the summit region localized at  $\theta = 90^\circ$ , and minimum value in the low part of annular space localized at  $\theta = 11^\circ$  and  $\theta = 169^\circ$ . On the internal wall, the variation of the local Nusselt number is reversed. Such oppositions find whatever the geometry studied and are explained if we know the distributions of the isothermal lines and streamlines. If the point of the wall is just situated between two contrarotating swirls, the local Nusselt number is minimum value if the fluid moves away from the wall and, maximum value at the corner joining the differentially heated isothermal walls  $\theta = 0^\circ$  and  $\theta = 180^\circ$ , what justified the analytical conduction solution [12].

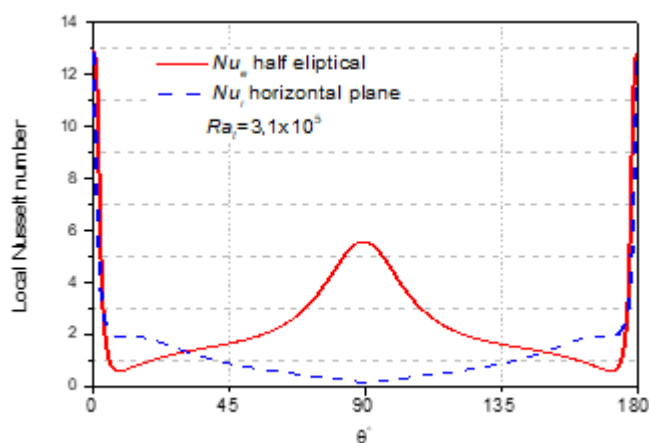


**Fig. 9.** Variation of the local Nusselt number along the internal and external walls

#### 4.5 Average Nusselt number

Figure 10 presents the evolution of the average Nusselt number. According to these results, it has been observed that the values of the average Nusselt number increase by increasing the value of the thermal Rayleigh number, which is obvious. The heat transfer is essentially conductive when the Rayleigh number is small.

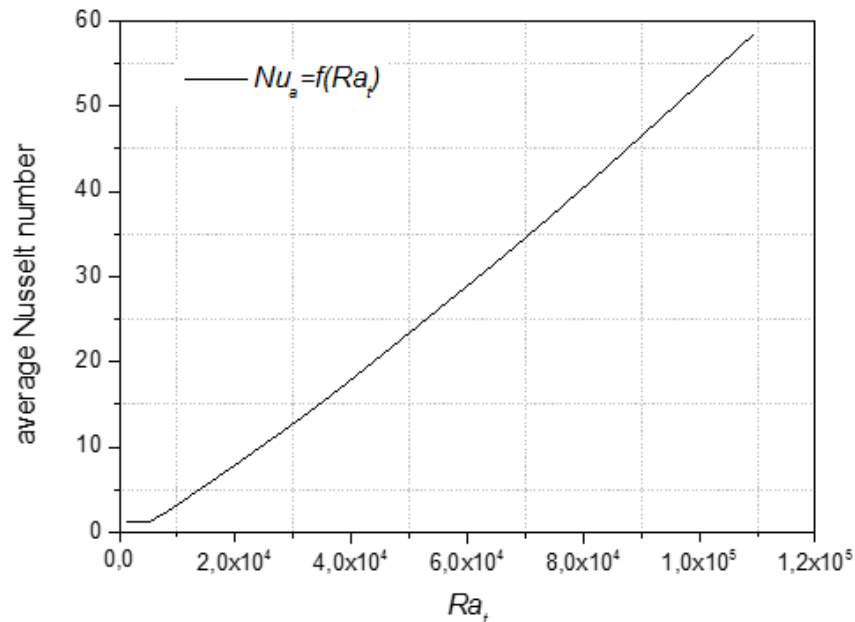


Fig. 10. Variation of the average Nusselt number

#### 5. Conclusion

In this paper, we have studied the behaviour of flow structures, the distributions of temperature in horizontal half-elliptic cavity. We noticed that the temperature distribution varies considerably according to the numbers of thermal Rayleigh. The structure of the flow is bicellular. The thermal stratification was developed in the middle of the cavity, and in similar way. The obtained results confirm that for a small thermal Rayleigh number, the heat transfer within the annulus is essentially controlled by the conduction process. As the thermal Rayleigh number increases ( $Ra_t \geq 10^4$ ), the role of convection becomes predominant. The local and average Nusselt numbers increase with the increase of the thermal Rayleigh number. The local Nusselt number is important in the two corners of the system (bigger to the extremes of half-ellipse) and small on the remainder. On the cold wall the maximum value of the local Nusselt number is reached at the angular position ( $\theta = 0^\circ$ ,  $\theta = 90^\circ$ , and  $\theta = 180^\circ$ ). These results will be used for the design of solar air heating system.

#### References

- [1] Aydin, Orhan, Ahmet Unal, and Teoman Ayhan. "A numerical study on buoyancy-driven flow in an inclined square enclosure heated and cooled on adjacent walls." *Numerical Heat Transfer: Part A: Applications* 36, no. 6 (1999): 585-599.
- [2] Rahman, M., and M. A. R. Sharif. "Numerical study of laminar natural convection in inclined rectangular enclosures of various aspect ratios." *Numerical Heat Transfer: Part A: Applications* 44, no. 4 (2003): 355-373.
- [3] Dalal, Amaresh, and Manab Kumar Das. "Natural convection in a rectangular cavity heated from below and uniformly cooled from the top and both sides." *Numerical Heat Transfer, Part A: Applications* 49, no. 3 (2006): 301-322.

- [4] Moukalled, F., and S. Acharya. "Natural convection in a trapezoidal enclosure with offset baffles." *Journal of Thermophysics and Heat Transfer* 15, no. 2 (2001): 212-218.
- [5] Deng, Qi-Hong, and Juan-Juan Chang. "Natural convection in a rectangular enclosure with sinusoidal temperature distributions on both side walls." *Numerical Heat Transfer, Part A: Applications* 54, no. 5 (2008): 507-524.
- [6] Sarris, I. E., I. Lekakis, and N. S. Vlachos. "Natural convection in a 2D enclosure with sinusoidal upper wall temperature." *Numerical Heat Transfer: Part A: Applications* 42, no. 5 (2002): 513-530.
- [7] Oztop, Hakan F., Yasin Varol, Ahmet Koca, and Mujdat Firat. "Experimental and numerical analysis of buoyancy-induced flow in inclined triangular enclosures." *International Communications in Heat and Mass Transfer* 39, no. 8 (2012): 1237-1244.
- [8] Anandalakshmi, R., Ram Satish Kaluri, and Tanmay Basak. "Heatline based thermal management for natural convection within right-angled porous triangular enclosures with various thermal conditions of walls." *Energy* 36, no. 8 (2011): 4879-4896.
- [9] Khubeiz, Jawad M., Ewa Radziemska, and Witold M. Lewandowski. "Natural convective heat-transfers from an isothermal horizontal hemispherical cavity." *Applied Energy* 73, no. 3-4 (2002): 261-275.
- [10] Baïri, Abderrahmane, and JM García de María. "Numerical and experimental study of steady state free convection generated by constant heat flux in tilted hemispherical cavities." *International Journal of Heat and Mass Transfer* 66 (2013): 355-365.
- [11] Saber, Hamed H., and Abdelaziz Laouadi. "Convective Heat Transfer in Hemispherical Cavities with Planar Inner Surfaces." *Ashrae Transactions* 117, no. 2 (2011).
- [12] Aydin, Orhan, and Gurkan Yesiloz. "Natural convection in a quadrantal cavity heated and cooled on adjacent walls." *Journal of Heat Transfer* 133, no. 5 (2011): 052501.
- [13] Yesiloz, Gurkan, and Orhan Aydin. "Natural convection in an inclined quadrantal cavity heated and cooled on adjacent walls." *Experimental Thermal and Fluid Science* 35, no. 6 (2011): 1169-1176.
- [14] Bose, Probir, Dipak Sen, Rajsekhar Panua, Ajoy Das, and Pulak Sen. "Laminar natural convection study in a quadrantal cavity using heater on adjacent walls." *Frontiers in Heat and Mass Transfer (FHMT)* 4, no. 1 (2013).
- [15] Retiel, N. and al. (2005). "Effect of the slope on the natural convection in an half-cylindrical cavity" *12èmes Journées Internationales de Thermique*. Tanger, Maroc du 15 au 17 Novembre.